WATER STATUS EVALUATION OF MAIZE CULTIVARS USING AERIAL IMAGES[1]

ADERSON SOARES DE ANDRADE JUNIOR[2]*, EDSON ALVES BASTOS[2], CARLOS ANTONIO FERREIRA DE SOUSA[2], RAPHAEL AUGUSTO DAS CHAGAS NOQUELI CASARI[3], BRAZ HENRIQUE NUNES RODRIGUES[4]

ABSTRACT – The objective of this study was to evaluate the water status of maize cultivars through thermal and vegetation indexes generated from multispectral aerial images obtained from an unmanned aerial vehicle (UAV), and correlate them with physiological indicators and soil water contents. The application of three water regimes based on the reference evapotranspiration (ETo) (30%, 90%, and 150% ETo) was evaluated for two maize cultivars (AG-1051 and BRS-Caatingueiro). An UAV was used to acquire thermal and multispectral images. The indexes evaluated were CWSI, CI-G, CI-RE, CIV, NDVI and OSAVI, which were correlated with gas exchange and soil moisture measures. The CWSI present correlation with physiological indicators (stomatal conductance, transpiration, and net CO_2 assimilation rate) that can be used to evaluate water status of maize plants. The multispectral vegetation indexes NDVI and OSAVI can replace the CWSI thermal index in water status evaluations for maize plants.

Keywords: *Zea mays* L.. ARP. Remote sensing. RGB imagens.

AVALIAÇÃO DO ESTADO HÍDRICO DE CULTIVARES DE MILHO POR IMAGENS AÉREAS

RESUMO – O estudo objetivou avaliar o estado hídrico de cultivares de milho por meio de índices térmico e de vegetação gerados de imagens aéreas multiespectrais obtidas por veículo aéreo não tripulado, correlacionando-os com indicadores fisiológicos e o conteúdo de água no solo. Avaliou-se a aplicação de três regimes hídricos (RH) com base na evapotranspiração de referência (ETo) (30%, 90% e 150% ETo) em duas cultivares de milho (AG-1051 e BRS-Caatingueiro). Utilizou-se um veículo aéreo não tripulado para a aquisição das imagens térmicas e multiespectrais. Avaliaram-se os índices CWSI, CI-G, CI-RE, CIV, NDVI e OSAVI, os quais foram correlacionados com medidas de trocas gasosas e umidade do solo. O CWSI apresenta correlação com os indicadores fisiológicos condutância estomática, transpiração e taxa de assimilação líquida de CO_2, podendo ser utilizado na avaliação do status hídrico de plantas de milho. Os índices de vegetação multiespectrais NDVI e OSAVI podem ser utilizados em substituição ao índice térmico CWSI na avaliação do estado hídrico das plantas de milho.

Palavras-chave: *Zea mays* L.. ARP. Sensoriamento remoto. Imagens RGB.

INTRODUCTION

Water is an important factor that limits grain yield in maize crops. Maize plants have C4 photosynthetic metabolism, with high efficiency in solar radiation use under adequate soil water availability. The more critical period for water deficit in maize plants is from the pre-flowering to the beginning of grain filling (BERGAMASCHI; MATZENAUER, 2014).

The canopy temperature is a water stress indicator in plants, which has been measured using portable thermographic cameras (BIAN et al., 2019; CASARI et al., 2019). Canopy temperature has significant negative correlation with maize yield (ROMANO et al., 2011). Maize genotypes selected as tolerant to water stress present lower canopy temperature and higher leaf stomatal conductance (ROMANO et al., 2011; ZIA et al., 2013), indicating that the thermography can be applied to studies on tolerance to water stress (CASARI et al, 2019).

The most used thermal index in thermography studies is the Crop Water Stress Index (CWSI) proposed by Idso et al. (1981), which correlates the difference between leaf and air temperatures with the vapor pressure deficit of the atmosphere. Some studies indicate promising results in plant water stress evaluations using CWSI (BIAN et al., 2019).

Proximal remote sensing stands out among the viable tools to remotely detect water stress in plants by thermography, but is not easily used for measurements at large scale. Thus, the use of thermal imaging of plants using unmanned aerial vehicles (UAV) is recommended (BIAN et al., 2019). It provides good results in terms of spatial resolution of images, flexible revisitation time, and high versatility under adverse climatic conditions (TORRES-SANCHEZ; LOPEZ-GRANADOS; PEÑA, 2015).

The remote detection by thermal infrared using UAVs has been widely practiced in agriculture to evaluate water stress in crops and irrigation managements (BERNI et al., 2009; GAGO et al., 2015; BELLVERT et al., 2016). Studies have indicated correlation between CWSI obtained from thermal images and physiological measurements, including stomatal conductance, transpiration rate, and soil water content (PADHI; MISRA; PAYERO, 2012; BELLVERT et al., 2014; GERHARDS et al., 2016).

Some vegetation indexes obtained from multispectral images are correlated to the water status of crops (GAGO et al., 2015). Vegetation indexes obtained from multispectral images, such as NDVI and OSAVI, are significantly correlated to water stress indicators in plants, such as stomatal conductance (BALUJA et al., 2012). However, validate the application of multispectral indexes using physiological and thermal indicators of plant water status is still required (BIAN et al., 2019), and

should be focused on substitute aerial thermography, much more expensive, by multispectral indexes obtained from RGB cameras that have lower costs.

In this context, the objective of this study was to evaluate the water status of maize cultivars through thermal and vegetation indexes generated from multispectral aerial images obtained by an UAV, and correlate them with physiological indicators and soil water contents, focused on substitute aerial thermography, which is an expensive method, by multispectral indexes obtained from RGB cameras, which has a lower cost.

MATERIAL AND METHODS

The study was conducted in the experimental station of the Embrapa Mid-North, in Parnaíba, PI, Brazil (03°04'14.3"S; 41°47'12.3"W, and 52 m of altitude). The aerial images were obtained from an experiment that evaluated the productive performance of maize cultivars in response the different water regimes (Figure 1).

The climate of the region is sub-humid dry, megathermal, with moderate water surplus in the summer and 30% concentration of potential evapotranspiration from October to December (BASTOS et al., 2018). The climatic conditions at the day (November 23, 2018) and time (between 10:00h and 12:00h) of the flights were: air temperature = 33.6 °C, relative air humidity = 42.0%, wind speed = 3.8 m s^{-1}, and solar radiation = 567.5 W m^{-2}. The data were obtained from an automatic meteorological station at 400 m from the area experimental.

The soil of the experimental area was classified as a Typic Hapludox (Latossolo Amarelo distrofico) of sandy texture (sand = 856.0 g kg^{-1}, silt = 62.0 g kg^{-1}, and clay = 82.0 g kg^{-1}), with water content at field capacity of 20.0% (volume) and density of 1.65 g cm^{-3} (MELO et al., 2004). Soil fertilizers were applied according to a previous soil analysis and following the recommendations for the crop (CARDOSO et al., 2012).

The experiment was conducted with maize plants irrigated by a fixed conventional sprinkler system, with sprinklers spaced 12 × 12 m apart. The application of three water regimes based on the reference evapotranspiration (ETo) (30%, 90%, and 150% ETo) was evaluated for two maize cultivars: AG-1051 (hybrid) and BRS-Caatingueiro (variety). These WR were applied using different irrigation times. The Penman-Monteith method was used to the estimate the reference evapotranspiration (ETo) (ALLEN et al., 1998). The total water depths of the irrigation applied in each WR, from sowing to the evaluation time, were 351.3 mm (30% ETo), 496.6 mm (90% ETo), and 641.9 mm (150% ETo).
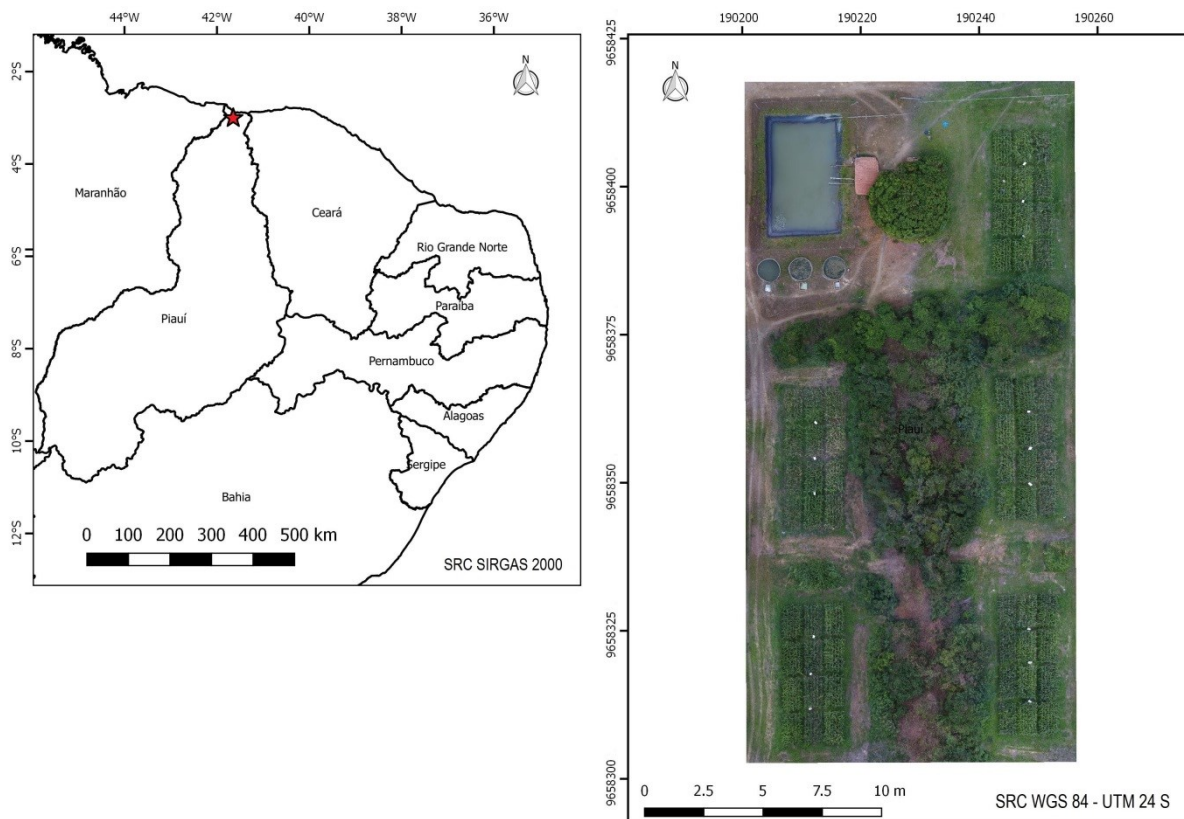
Figure 1. Location of the study area in the municipality of Parnaíba, Piauí, Brazil (left) and aerial digital image of the experimental area grown with maize under different water regimes (right). Embrapa Mid-North, Parnaíba, PI, Brazil.

A randomized block experimental design was used, with three treatments arranged in split-plot, with the WR in the plots, and the cultivars in the subplots, and four replications. The maize seeds were sowed with spacing of 0.5 m between rows, and four plants per meter (10 plants m^{-2}). The subplot consisted of six 5-meter rows (15 m^2); the four central rows were used for the evaluations (10 m^2). The size of the experimental plots was 30 m^2. The sowing was carried out on September 26, 2018, and the harvest (dry grains) on January 16, 2019 (BRS-Caatingueiro) and January 21, 2019 (AG-1051).

The images were acquired using an unmanned aerial vehicle (UAV), a X800 XFLY Brasil hexacopter (XFly Brasil, Bauru, Brazil). Two flights were carried out on November 23, 2018, 58 days after the maize sowing (DAS), between 10:00 and 12:00 hours: one for acquisition of multispectral, and other for thermographic images. The flight for capture multispectral images was planned using the Mission Planner software. The flight plan was created ensuring that the capture of images created a minimum lateral and frontal overlap of 75%, maintaining the flight line at 40 meters above ground level.

The multispectral images were acquired using a sensor RedEdge® (MicaSense), which captures five spectral bands, simultaneously: Red (668 nm), Green (560 nm), Blue (475 nm), NIR (840 nm), and

RedEdge (717 nm). The images were georeferenced for correction using a GPS and a solar radiation sensor installed in the upper part of the UAV. A radiometric calibration standard was used for the correction of the images. The images were saved in 16-bit TIFF files. The image orthomosaic was developed using the Pix4D Mapper® software.

Thermographic images were acquired using a FLIR T-420® sensor (FLIR Systems, Danderyd, Sweden), which presents spatial resolution of 320 × 240, spectral response of 7.5 to 13 μm, non-refrigerated microbolometer, frame rate of 60 Hz, thermal sensitivity of 0.045 °C to 30 °C, accuracy of ±2 °C or 2% (whichever is higher), 25° lens, and weight of 0.88 kg, including the battery.

The camera was set for the environmental conditions at the time of capture of the image following the thermography bases presented by Usamentiaga et al. (2014), which include environmental air temperature, distance from the target object, emissivity of the target object, reflected temperature, and relative air humidity. The thermographic images were saved in radiometric JPEG files.

Five vegetation indexes were evaluated; they were estimated using bands of multispectral indexes (R, G, B, Red-Edge, and NIR), and a thermal index (CWSI) (Table 1). The multispectral indexes were estimated using the raster calculator of the QGIS software (QGIS, 2016). The vegetation indexes of

each subplot were extracted using the zonal statistics plugin of the QGIS software (QGIS, 2016). This process was carried out using the shapefile of the experimental subplots, consisted of the four central rows (10 m^2).

The CWSI was evaluate using estimates of hot pixels (Td) considering the mean of the 5% highest leaf temperatures extracted from the temperature histogram of the subplot. The mean of 5% lower leaf temperatures extracted from the temperature histogram of the subplot was used for the cold pixels. Tc was estimated considering the mean leaf temperature of the subplot. Only temperatures of pixels classified as leaves were used for the estimates, i.e., excluding pixels classified as soil (BIAN et al., 2019).

Table 1. Vegetation indexes and the thermal index evaluated.

Indexes	Abbreviation	Equation	Reference
Chlorophyll index–green	CI-G	$= \dfrac{R_n}{R_g} - 1$	Escadafal (1994)
Chlorophyll index – Red Edge	CI-RE	$= \dfrac{R_n}{R_{RE}} - 1$	Gitelson et al. (2003)
Chlorophyll vegetation index	CVI	$= \dfrac{R_n R_r}{R_g{}^2}$	Vincini, Frazzi and D'Alessio (2008)
Normalized Difference Vegetation Index	NDVI	$= \dfrac{R_n - R_r}{R_n + R_r}$	Gitelson et al. (2003)
Optimized Soil Adjusted Vegetation Index	OSAVI	$= \dfrac{R_n - R_r}{R_n + R_r + 0,16}$	Roundeaux, Steven and Baret (1996)
Crop Water Stress Index	CWSI	$= \dfrac{T_c - T_d}{T_w - T_d}$	Idso et al. (1981)

Rn: Spectral reflectance – near infrared (840 nm); Rg: spectral reflectance – green (560 nm); RRE: spectral reflectance – near red (717 nm); Rr: spectral reflectance red (668 nm); Tc: mean canopy leaf temperature (°C); Td: mean hot pixel temperature (°C); Tw: mean cold pixel temperature (°C).

Soil pixels were removed from the thermal images using the image segmentation process described by Otsu (1979) available in the ImageJ software (FERREIRA; RASBAND, 2012). This method estimates an ideal threshold that separates the pixels of the image into two classes (soil and leaves); similar procedure was adopted in other studies (MONTALVO et al., 2012; BANGARE et al., 2015).

Gas exchange was measured using a portable gas analyzer that reads the infrared region of the electromagnetic spectrum (6400XT; LI-COR, Lincoln, USA), which has a measurement chamber with an artificial illumination system (6400-02B; LI-COR, Lincoln, USA). The device was set to maintain a relative air humidity of 50% to 60% inside the measurement chamber, with temperature of the block adjusted to 35 °C. The light intensity inside the measurement chamber was set to 2000 µmol m^{-2} s^{-1}, with air flow rate of 400 µmol s^{-1}, and CO_2 concentration of 400 ppm in the cell of reference, using a CO_2 6400-01 mixer with a CO_2 cylinder of 12 g. The measures were done in one plant per subplot, using the mid third of the leaf of the ear. The data extracted by the Open 6.3 program were: net CO_2 assimilation rate (µmol CO_2 m^{-2} s^{-1}), stomatal conductance at water vapor (mmol H_2O m^{-2} s^{-1}), and transpiration rate (mmol H_2O m^{-2} s^{-1}).

The soil water content was quantified by the gravimetric method, with drying of soil samples in an oven at 105 °C until constant weight. Undisturbed soil samples were collected from the 0-0.2 and 0.2-0.4 m layers, with three replications in each water regime. The collections were carried out just before the acquisition of the aerial images.

The data obtained were subjected to the Shapiro-Wilk (normality of errors) and Cochran T (homogeneity of variance) tests. Satisfied these basic requirements, the data were subjected to analyses of variance, comparison of means (Tukey), and Pearson's correlation (t test) between vegetation and thermal indexes and the gas exchange measures (net CO_2 assimilation rate, stomatal conductance, and transpiration). The statistical analyses were carried out using the ExpDes.pt package of the R program (FERREIRA; CAVALCANTI; NOGUEIRA, 2014).

RESULTS AND DISCUSSION

Canopy temperature, CWSI, and soil moisture

The canopy temperature (Tc) presented significant response to the water regimes (WR), cultivars (C), and to the interaction between WR and cultivars. The interaction between CWSI and cultivars was not significant (Table 2), indicating the capacity of the thermal image to detect the water status of maize plants. This detection capacity was sensitive to the maize cultivars. Casari et al. (2019) proposed the use of thermal images for phenotyping

of maize genotypes for tolerance to soil water deficit and concluded that thermography can discriminate contrasting maize genotypes for tolerance to water deficit similarly to field phenotyping, which considers only the grain yield as the criterion.
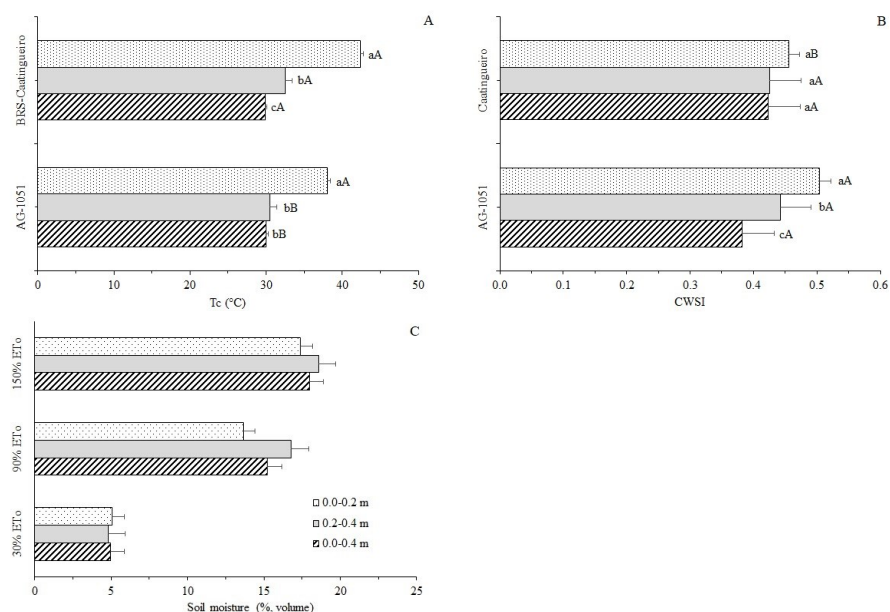
The mean canopy temperature (Tc) of both cultivars evaluated decreased as the soil water availability was increased due to the application of the water regimes (Figure 2A). The cultivar AG-1051 presented no significant difference (p<0.01) for Tc in the WR of 90% ETo (30.5 °C) and 150% ETo (30.0 °C); however, the WR of 30% ETo (38.9 °C) presented a significant variation. The cultivar BRS-Caatingueiro presented significant variation (p<0.01) for Tc values in all WR evaluated,

indicating that this cultivar present higher leaf thermal plasticity, which allows it to respond to different soil water availability conditions. The cultivar BRS-Caatingueiro is characterized by a very-early cycle (90-100 days), flowering at approximately 45 days after sowing, and high production stability in environments with low water availability, such as semiarid regions (CARVALHO et al., 2004). Contrastingly, the cultivar AG-1051 is a hybrid that present high water use efficiency, which can be due to a physiological mechanism (stomatal closure) in soil water deficit conditions (SOUSA et al., 2015), which decreases transpiration and internal CO_2 concentration (TAIZ et al., 2017).

Table 2. Analysis of variance for canopy temperature and CWSI in response at water regimes and maize cultivars evaluated.

Source of variation	Degrees of freedom	Mean canopy leaf temperature (Tc)		Crop water stress index (CWSI)	
Water regimes (WR)	3	246.695	***	0.0121	*
Blocks	2	0.567		0.0012	
Error a	1	0.429		0.0012	
Cultivars (C)	2	25.309	***	0.0004	ns
WR × C	15	9.929	***	0.0041	°
Error b	9	0.573		0.0011	
CV - WR (%)		1.933		7.902	
CV - C (%)		2.234		7.382	

*** = significant by the F test at ≤0.001; * = significant by the F test at ≤0.05; ° = significant by the F test at ≤0.1; ns = not significant.

Lowercase letters compare means within the same cultivar and uppercase letters compare cultivars by the Tukey's test at 5% significance level.

Figure 2. Mean canopy temperature (Tc) (A), thermal index (CWSI) (B), and soil moisture (C) response to the application of three water regimes (30%, 90% and 150% ETo) for two maize cultivars (BRS-Caatingueiro and AG-1051). Parnaíba, PI, Brazil.

It was not possible to distinguish the different water status of maize plants of the variety BRS-Caatingueiro by the CWSI, despite they were subjected to different soil water availabilities (5.0% the 18.0% moisture) in the 0-0.4 m layer (Figures 2B, 2C). However, the different water status of maize plants of the cultivar AG-1051 were detected by the CWSI, which were 0.505 (30% ETo), 0.442 (90% ETo) and 0.383 (150% ETo) (Figure 2B). This trend confirms the higher tolerance to soil water deficit of the cultivar BRS-Caatingueiro when compared to the AG-1051.

The CWSI was significant different (p<0.01) between the two genotypes only under the lowest soil water availability conditions (30% ETo) (Figure 2B). The cultivar AG-1051 presented higher CWSI (0.505) than the BRS-Caatingueiro (0.456) due to a better physiological regulation of the variety when compared to the hybrid in low soil water availability conditions (TAIZ et al., 2017; SOUSA et al., 2015). Taghvaeian, Chávez and Hansen (2012) found high correlation between CWSI and soil water contents, especially in more surface layers, for maize plants subjected to different water regimes. Moreover, Bian

et al. (2019) found that CWSI can better characterize the water status of cotton plants subjected to high soil water availability conditions, which did not occur when the plants were subjected to soil water deficit; this indicate that the CWSI is affected by the physiological system of the evaluated plants.

Correlation between gas exchange, CWSI, and multispectral indexes

The gas exchange variables (stomatal conductance, net CO_2 assimilation rate, and transpiration) were significantly affected (p<0.01) by the water regimes used. The gas exchange variables were not affected by the cultivars, nor by the interaction between water regimes and cultivars (Table 3). However, physiological changes in stomatal conductance, net CO_2 assimilation rate, and transpiration in maize plants subjected to full and deficit irrigation were detected in other studies (BIANCHI et al., 2007; RIBOLDI, OLIVEIRA; ANGELOCCI, 2016; SABAGH; BARUTÇULAR; ISLAM, 2017).

Table 3. Analysis of variance for the response of gas exchange variables to water regimes and maize cultivars.

Source of variation	Degrees of freedom	gs		E		A	
Water regimes (WR)	3	0.076	***	26.703	***	515.660	***
Blocks	2	0.002	ns	0.465	ns	25.830	ns
Error a	1	0.001		0.208		11.900	
Cultivars (C)	2	0.000	ns	0.109	ns	12.310	ns
WR × C	2	0.001	ns	0.835	ns	4.080	ns
Error b	9	0.001		0.438		13.120	
Total	23						
CV - WR (%)		13.756		5.591		11.208	
CV - C (%)		14.024		8.120		11.772	

A = net CO_2 assimilation rate (μmol CO_2 m^{-2} s^{-1}); gs = stomatal conductance (mmol H_2O m^{-2} s^{-1}); E = transpiration rate (mmol H_2O m^{-2} s^{-1}); CV = coefficient of variation; *** = significant by the F test at ≤ 0.001; ns = not significant.

The increase in soil water availability caused by the application of water regimes increased the stomatal conductance (gs) (Figure 3A), which was more pronounced between the extreme water regimes (30 and 150% ETo), with 0.13 mol H_2O m^{-2} s^{-1} (30% ETo) and 0.30 mol H_2O m^{-2} s^{-1} (150% ETo). The difference in stomatal conductance between the regimes of 90% and 150% ETo was not significant (p>0.05), presenting a mean of 0.305 mol H_2O m^{-2} s^{-1} (Figure 3A). Similar results were found by Bianchi et al. (2007), who evaluated the effect of different irrigation levels in maize crops under no-tillage and conventional systems, with the highest stomatal conductance values under full irrigation (0.35 to

0.60 mmol H_2O m^{-2} s^{-1}), and the lowest under water deficit (0.12 to 0.20 mmol H_2O m^{-2} s^{-1}). Sabagh, Barutçular and Islam (2017) evaluated the physiology of maize cultivars under full and deficit irrigation regimes and found mean values of 0.30 mmol H_2O m^{-2} s^{-1} for the full irrigation and 0.15 mmol H_2O m^{-2} s^{-1} for the deficit irrigation.

Higher stomatal conductance values are found when the solar radiation is high and the leaf water potential has not yet reached the minimum values to induce stomatal closure. Plants tend to decrease stomatal conductance under water deficit conditions as a strategy to avoid water loss to the atmosphere (RIBOLDI, OLIVEIRA; ANGELOCCI, 2016; SANTOS et al., 2018).
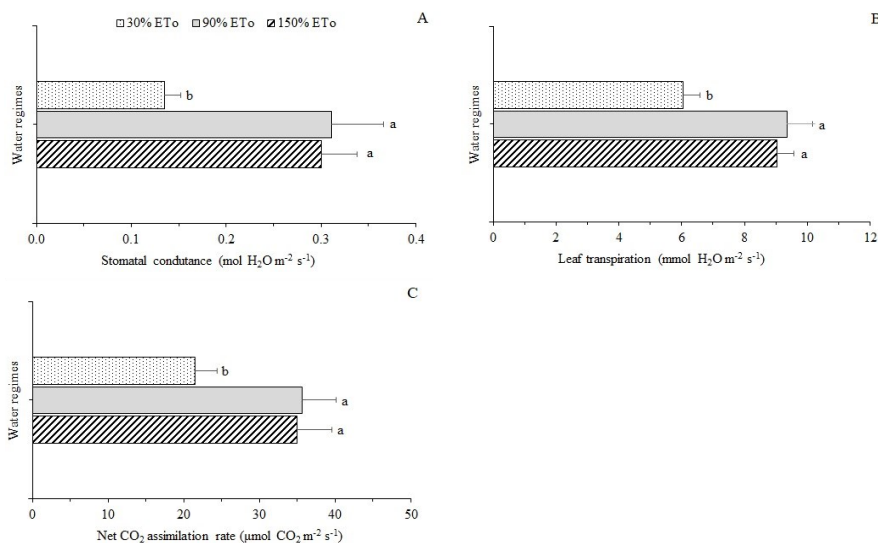
A: stomatal conductance; B: leaf transpiration; C: net CO_2 assimilation rate.
Means followed by the same letter are not different by the Tukey's test at 5% significance level.

Figure 3. Gas exchange responses to application of three water regimes (30%, 90% and 150% ETo). Parnaíba, PI, Brazil.

Decreases in soil water availability decrease the transpiration rate of plants. The transpiration rates found under high soil water availability were 9.35 mmol H_2O m^{-2} s^{-1} (90% ETo) and of 9.03 mmol H_2O m^{-2} s^{-1} (150% ETo), whereas that found under soil water deficit was 6.05 mmol H_2O m^{-2} s^{-1} (30% ETo) (Figure 3B). Martins (2010) found transpiration rates of 8.0 to 12.0 mmol H_2O m^{-2} s^{-1} for the maize cultivar Pioneer 32R22-H grown under high soil water availability conditions.

The decrease in transpiration rates is more expressive under soil water deficit conditions. Decreases in transpiration rate is a response of the stomatal conductance to decreases in soil water availability, mainly for plants subjected to only 30% of the crop water requirement (Figure 3A). Decreases in soil water availability to plants tend to decrease stomatal conductance and, consequently, transpiration rate (LIU et al., 2011).

This physiological response is important because decreases the photosynthetic rates, which negatively affects grain production (TAIZ et al., 2017). Bianchi et al. (2007) evaluated changes in leaf stomatal conductance in maize crops grown under different soil water availabilities and found that treatments with irrigations close to the field capacity present higher transpiration rates.

The stomatal conductance and transpiration rates found as responses to soil water availability directly affected the net CO_2 assimilation rate (Figure 3C), indicating a direct correlation between them. The highest net CO_2 assimilation rates were found for the highest soil water availability conditions, similarly to the dynamic found for stomatal conductance and transpiration rate.

The net CO_2 assimilation rate varied from 35.6 μmol CO_2 m^{-2} s^{-1} (150% ETo) to 35.7 μmol CO_2 m^{-2} s^{-1} (90% ETo) under high soil water availability conditions, and 21.5 μmol CO_2 m^{-2} s^{-1} when using only 30% ETo (Figure 3C). Net CO_2 assimilation rates of 30.0 μmol CO_2 m^{-2} s^{-1} under full irrigation regime, and 22.0 μmol CO_2 m^{-2} s^{-1} under deficit irrigation were found for the maize cultivar AG-5055 (RIBOLDI; OLIVEIRA; ANGELOCCI, 2016).

The net CO_2 assimilation rate in plants is affected by water stress caused by changes in the leaf water potential (GHANNOUM, 2009). Maize plants subjected to water deficit show low leaf water potential, causing stomatal closure (decrease stomatal conductance) and, therefore, decrease net CO_2 assimilation rate (OTEGUI; ANDRADE; SUERO, 1995).

Regarding the genotypes evaluated, no significant variation was found for stomatal conductance, net CO_2 assimilation rate, and transpiration rate due to the different soil water availabilities (Table 3). The cultivar BRS-Caatingueiro was expected to have higher tolerance to water deficit, with different rates when compared to the AG-1051, mainly under the most pronounced water deficit conditions, but it was not found in the present study. Avila et al. (2016) evaluated the response of sensitive (BRS1010 and 2B710) and tolerant (DKB390 and BRS1055) maize genotypes to water deficit, with different irrigation regimes (full and deficit irrigation) and also found no significant differences (p>0.05) in stomatal conductance and transpiration rates between the genotypes under

deficit irrigation condition. However, they reported that the net CO_2 assimilation rate was different between the genotypes, with higher rates for the genotypes more tolerant to water deficit.

The CWSI presented linear negative correlation to stomatal conductance, transpiration rate, and net CO_2 assimilation rate for both the genotypes evaluated, with values between -0.752 and -0.887 (Figures 4A to 4C). These negative values indicate that stomatal conductance, transpiration rate, and net CO_2 assimilation rate decrease as the CWSI is increased; these physiological dynamics is adequate and coherent with the thermal response of the crop canopy. Bian et al. (2019) found negative linear correlation between CWSI and stomatal conductance (R = -0.66, p<0.01) and transpiration (R = -0.596, p<0.01) for cotton crops subjected to different water regimes.

Negative linear correlation between CWSI and stomatal conductance in maize cultivars was found by Zia et al. (2013), with values of 0.72 to 0.81, which are similar those found in the present study. They concluded that the genotypes selected as the most tolerant to water stress, considering the grain yield, presented lower canopy temperature, lower CWSI, and higher stomatal conductance.

Regarding the correlation between CWSI and multispectral vegetation indexes, the coefficients of correlation varied from 0.468 (CVI) to -0.852 (OSAVI) (Figure 5). An inverse linear correlation was found between CWSI and all indexes, except CVI. The correlation between CWSI and the indexes NDVI (0.763; p<0.001) and OSAVI (0.852; p<0.001) presented high R values, indicating that these indexes present potential for the evaluation of water status of maize plants as well as the CWSI.
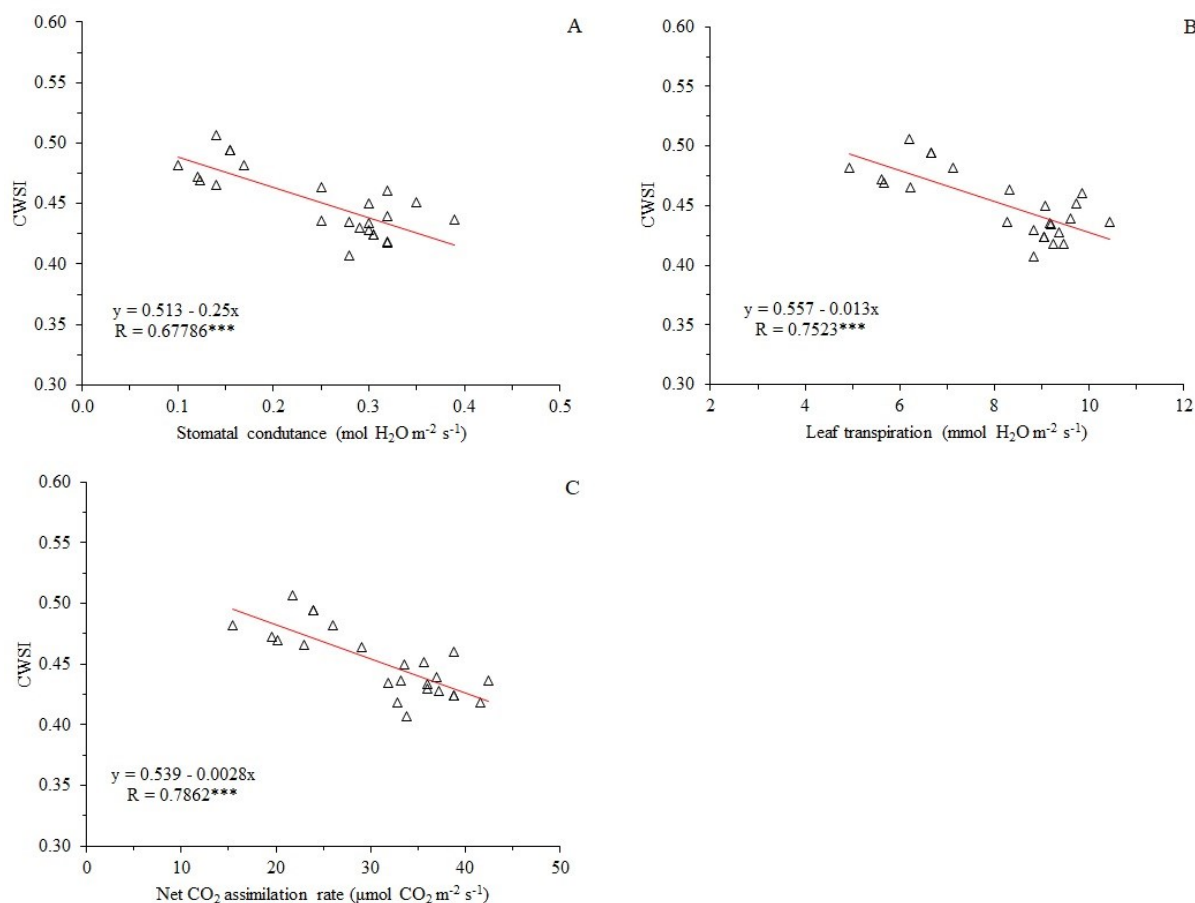
A: transpiration leaf; B: stomatal conductance; C: net CO_2 assimilation rate
***significance level by the t test: ≤ 0.001.

Figure 4. Pearson's correlation between CWSI and gas exchange of maize cultivars under application of different water regimes. Parnaíba, PI, Brazil.
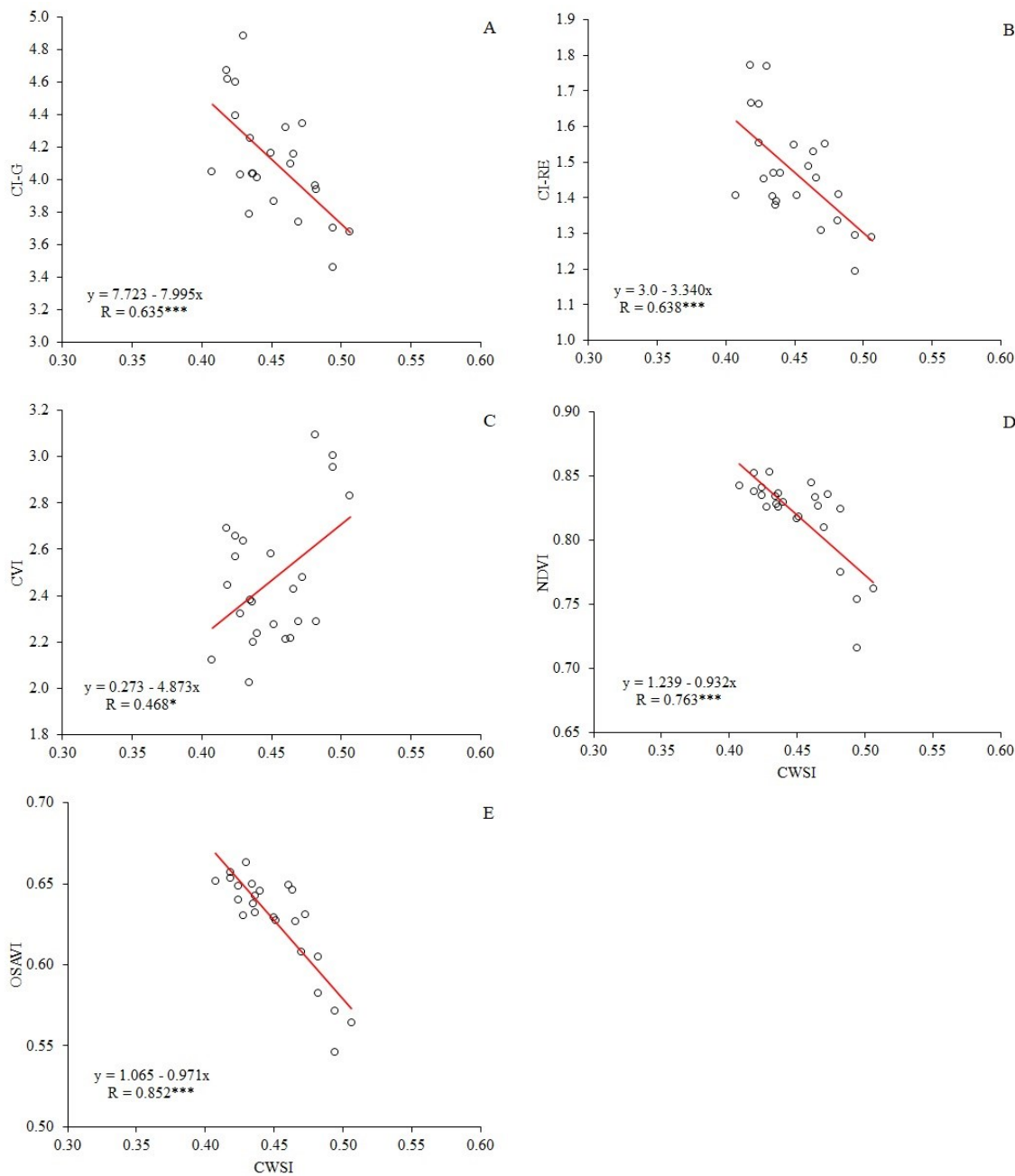
A: CI-G (chlorophyll index – green); B: CI-RE (chlorophyll index – Red Edge); C: CVI (chlorophyll vegetation index); D: NDVI (normalized difference vegetation index); E: OSAVI (Optimized soil adjusted vegetation index); significance levels by the t test: *** = ≤ 0.001, * = ≤ 0.05.

Figure 5. Pearson's correlation between CWSI and multispectral vegetation indexes of maize cultivars under application of different water regimes. Parnaíba, PI, Brazil.

Romano et al. (2011) used thermography to screen maize genotypes, focused on evaluating their tolerance to water deficit and found significant linear correlation between CWSI and NDVI (R = 0.58; p<0.01). Zhang et al. (2019) evaluated the potential of using multispectral vegetation indexes in remote detection of water status of maize plants compared to CWSI, and found significant negative linear correlations (p<0.001) between CWSI and the indexes NVDI (R = -0.845; p<0.001) and OSAVI (R = -0.859; p<0.001). This result confirms those

found in the present study, and indicate that these indexes have high potential for the evaluation of water status of maize plants. The literature also reports similar results for other crops (BALUJA et al., 2012; LI et al., 2013).

CONCLUSIONS

The CWSI present correlation with the

physiological indicators stomatal conductance, transpiration rate, and net CO_2 assimilation rate, and can be used for evaluations of water status of maize plants. The multispectral vegetation indexes NDVI and OSAVI can be used in substitution to the thermal index CWSI in evaluations of water status of maize plants, denoting the potential of using proximal remote sensing as a tool to remotely detect water stress in maize crops.

REFERENCES

ALLEN, R. G. et al. **Crop evapotranspiration**: Guidelines for computing crop water requirements. FAO Irrigation and Drainage Paper 56. FAO: Rome, 1998. 300 p.

AVILA, R. G. et al. Alterações nos componentes de trocas gasosas e eficiência do fotossistema II em genótipos de milho submetidos a estresse hídrico no pré-florescimento. In: CONGRESSO NACIONAL DE MILHO E SORGO, 31, 2016, Bento Gonçalves. **Anais...** Bento Gonçalves: SBMS, 2016. p. 642-644.

BALUJA, J. et al. Assessment of vineyard water status variability by thermal and multispectral imagery using an unmanned aerial vehicle (UAV). **Irrigation Science**, 30: 511-522, 2012.

BANGARE, S. L. et al. Reviewing Otsu's method for image thresholding. **International Journal of Applied Engineering Research**, 10: 21777-21783, 2015.

BASTOS, E. A. et al. **Boletim agrometeorológico de 2017 para o município de Parnaíba, PI**. Teresina, PI: Embrapa Meio-Norte, 2018. 37 p. (Documentos, 251).

BELLVERT, J. et al. Mapping crop water stress index in a 'pinot-noir' vineyard: Comparing ground measurements with thermal remote sensing imagery from an unmanned aerial vehicle. **Precision Agriculture**, 15: 361–376, 2014.

BELLVERT, J. et al. Vineyard irrigation scheduling based on airborne thermal imagery and water potential thresholds. **Australian Journal of Grape and Wine Research**, 22: 307–315, 2016.

BERGAMASCHI, H.; MATZENAUER, R. **O milho e o clima**. Porto Alegre, RS: Emater/RS-Ascar, 2014. 84 p.

BERNI, J. A. J. et al. Mapping canopy conductance and CWSI in olive orchards using high resolution thermal remote sensing imagery. **Remote Sensing of Environment**, 113: 2380–2388, 2009.

BIAN, J. et al. Simplified Evaluation of Cotton Water Stress Using High Resolution Unmanned Aerial Vehicle Thermal Imagery. **Remote Sensing**, 11: 267-284, 2019.

BIANCHI, C. A. M. et al. Condutância da folha em milho cultivado em plantio direto e convencional em diferentes disponibilidades hídricas. **Ciência Rural**, 37: 315-322, 2007.

CARDOSO, M. J. et al. **Rendimento de grãos, componentes de rendimento e eficiência de uso da água de híbridos de milho em condições climáticas contrastantes**. Teresina, PI: Embrapa Meio-Norte, 2012. 23 p. (Boletim de pesquisa e desenvolvimento, 103).

CARVALHO, H. W. L. et al. **Caatingueiro - Uma variedade de milho para o semiárido Nordestino**. Aracaju, SE: Embrapa Tabuleiros Costeiros, 2004. 5 p. (Comunicado técnico, 29).

CASARI, R. A. C. N. et al. Using thermography to confirm genotypic variation for drought response in maize. **International Journal of Molecular Sciences**, 20: 2273-2295, 2019.

ESCADAFAL, R. Soil spectral properties and their relationships with environmental parameters: examples from arid regions. In: HILL, J.; MÉGIER, J. (Eds.). **Imaging Spectrometry-A Tool for Environmental Observations**. Dordrecht: Kluwer Academic Publishers, 1994. v. 4, cap. 5, p. 71-87.

FERREIRA, E.; CAVALCANTI, P.; NOGUEIRA, D. ExpDes: An R Package for ANOVA and Experimental Designs. **Applied Mathematics**, 5: 2952-2958. 2014.

FERREIRA, T.; RASBAND, W. S. **ImageJ User Guide** — IJ 1.46. National Institutes of Health, Bethesda, Maryland, USA, 2012. 198 p. Disponível em: <http://imagej.nih.gov/ij/ docs/guide>. Acesso em: 05 mai. 2019.

GAGO, J. et al. UAVs challenge to assess water stress for sustainable agriculture. **Agricultural Water Management**, 154: 9–19, 2015.

GERHARDS, M. et al. Water stress detection in potato plants using leaf temperature, emissivity, and reflectance. **International Journal of Applied Earth Observation and Geoinformation**, 53: 27-39, 2016.

GHANNOUM, O. C4 photosynthesis and water stress. **Annals of Botany**, 103: 635-644, 2009.

GITELSON, A. A. et al. Remote estimation of leaf area index and green leaf biomass in maize canopies.

Geophysical Research Letters, 30: 1248-1252, 2003.

IDSO, S. B. et al. Normalizing the stress-degree-day parameter for environmental variability. **Agricultural Meteorology**, 24: 45-55, 1981.

LI, H. et al. Estimating crop coefficients of winter wheat based on canopy spectral vegetation indices. **Transactions of Chinese Society of Agricultural Engineering**, 29: 118–127, 2013.

LIU, Y. et al. Maize leaf temperature responses to drought: Thermal imaging and quantitative trait loci (QTL) mapping. **Environmental and Experimental Botany**, 71: 158-165, 2011.

MARTINS, J. D. **Modificações morfofisiológicas em plantas de milho submetidas a déficit hídrico**. 2010. 102 p. Dissertação (Mestrado em Engenharia Agrícola: Área de Concentração em Engenharia de Água e Solo) – Universidade Federal de Santa Maria, 2010.

MELO, F. B. et al. **Levantamento Detalhado dos Solos da Área da Embrapa Meio-Norte / UEP de Parnaíba**. Teresina, PI: Embrapa Meio-Norte, 2004. 22 p. (Documentos, 89).

MONTALVO, M. et al. Automatic detection of crop rows in maize fields with high weeds pressure. **Expert System Applied**, 39: 11889–11897, 2012.

OTEGUI, M. E.; ANDRADE, F. H.; SUERO, E. E. Growth, water use, and kernel abortion of maize subjected to drought at silking. **Field Crop Research**, 40: 87–94, 1995.

OTSU, N. A threshold selection method from gray-level histograms. IEEE **Transactions on Systems, Man. and Cybernetics**, 9: 62–66, 1979.

PADHI, J.; MISRA, R. K.; PAYERO, J. O. Estimation of soil water deficit in an irrigated cotton field with infrared thermography. **Field Crops Research**, 126: 45–55, 2012.

QGIS Development Team, 2016. QGIS 2.18. **Geographic Information System User Guide**. Open Source Geospatial Foundation Project. Disponível em: <https://docs.qgis.org/ 2.18/pdf/ pt_BR/>. Acesso em: 01 nov. 2016.

RIBOLDI, L. B.; OLIVEIRA, R. F.; ANGELOCCI, L. R. Leaf turgor pressure in maize plants under water stress. **Australian Journal of Crop Science**, 10: 878-886, 2016.

ROMANO, G. et al. Use of thermography for high throughput phenotyping of tropical maize adaptation in water stress. **Computers and Electronics in Agriculture**, 79: 67–74, 2011.

RONDEAUX, G.; STEVEN, M.; BARET, F. Optimization of soil-adjusted vegetation indices. **Remote Sensing of Environment**, 55: 95-107, 1996.

SABAGH, A. E.; BARUTÇULAR, C.; ISLAM, M. S. Relationships between stomatal conductance and yield under deficit irrigation in maize (Zea mays L.). **Journal of Experimental Biology and Agricultural Sciences**, 5: 14-21, 2017.

SANTOS, A. L. F. et al. Eficiência fotossintética e produtiva de milho safrinha em função de épocas de semeadura e populações de plantas. **Journal of Neotropical Agriculture**, 5: 52-60, 2018.

SOUSA, R. S. et al. Desempenho produtivo de genótipos de milho sob déficit hídrico. **Revista Brasileira de Milho e Sorgo**, 14: 49-60, 2015.

TAGHVAEIAN, S.; CHÁVEZ, J. L.; HANSEN, N. C. Infrared thermometry to estimate crop water stress index and water use of irrigated maize in Northeastern Colorado. **Remote Sensing**, 4:3619-3637, 2012.

TAIZ, L. et al. **Fisiologia Vegetal**. 6. ed. Porto Alegre, RS: Artmed, 2017. 918 p.

TORRES-SANCHEZ, J.; LOPEZ-GRANADOS, F.; PEÑA, J. M. An automatic object-based method for optimal thresholding in UAV images: Application for vegetation detection in herbaceous crops. **Computers and Electronics in Agriculture**, 114: 43-52, 2015.

USAMENTIAGA, R. et al. Infrared thermography for temperature measurement and non-destructive testing. **Sensors**, 14: 12305–12348, 2014.

VINCINI, M.; FRAZZI, E.; D'ALESSIO, P. A broad-band leaf chlorophyll vegetation index at the canopy scale. **Precision Agriculture**, 9: 303–319, 2008.

ZHANG, L. et al. Mapping maize water stress based on UAV multispectral remote sensing. **Remote Sensing**, 11: 605-629, 2019.

ZIA, S. et al. Infrared thermal imaging as a rapid tool for identifying water-stress tolerant maize genotypes of different phenology. **Journal of Agronomy and Crop Science**, 199: 75-84, 2013.